

The Quantum Interference Effect Transistor

D. M. Cardamone, C. A. Stafford, S. Mazumdar

Department of Physics, University of Arizona, 1118 E. 4th Street, P. O. Box 210081, Tucson, AZ 85721

We propose a new type of molecular transistor, the Quantum Interference Effect Transistor (QuIET), based on tunable current suppression due to quantum interference. We show that any aromatic hydrocarbon ring has two-lead configurations for which current at small voltages is suppressed by destructive interference. A transistor can be created by providing phase relaxation or decoherence at a site on the ring. We propose several molecules which could tunably introduce the necessary dephasing or decoherence, as well as a proof of principle using a scanning tunneling microscope tip. Within the self-consistent Hartree-Fock approximation, the QuIET is shown to have characteristics strikingly similar to those of conventional field effect and bipolar junction transistors.

I. INTRODUCTION

Although there has been considerable scientific and commercial interest, a small molecular transistor has yet to be discovered. Needless to say, such a device is crucial to transferring existing technology to smaller length scales. Current industrial fabrication techniques have more or less exhausted the possibilities for purely classical phenomena to solve this problem. We must therefore turn to quantum mechanical effects in the search for smaller transistors. The solution, therefore, is also of fundamental interest to mesoscopic and molecular physicists: we find that the “small transistor” problem is an engaging way of posing the question, “What happens to multi-lead, many-body electronic systems when their size is such that quantum effects are important?”

We propose a new type of device, the Quantum Interference Effect Transistor (QuIET), capable of filling the role of the Field Effect Transistor (FET) and Bipolar Junction Transistor (BJT) at length scales $\lesssim 1\text{nm}$. The QuIET consists simply of a hydrocarbon ring and a mechanism to tunably introduce phase relaxation at a particular site. Unlike the Single Electron Transistor (SET), the transistor behavior can occur over a large range of base voltages. Its $I - \mathcal{V}$ characteristic is a single, broad resonance, strikingly similar to those of macroscopic transistors over a domain of several volts. This is to be taken in contrast to the SET’s $I - \mathcal{V}$, a series of many sharp peaks.

The operating principle of the QuIET is that bias applied to a third lead can modulate an otherwise complete conductance suppression across a hydrocarbon ring. This conductance suppression is a simple, single-particle effect of quantum mechanics. The modulation from a third lead can be achieved either through direct coupling to the molecule (Fig. 1a), as in the case of a scanning tunneling microscope (STM) tip, or via the introduction of an appropriate intermediary molecular complex, as shown in Fig. 1b. In either case, the resultant device is an excellent molecular-scale transistor.

Section II gives an outline of the extended Hubbard model Hamiltonian and Green function formalism we use to treat the problem. The multi-terminal current formula allows extraction of current. Section III explains

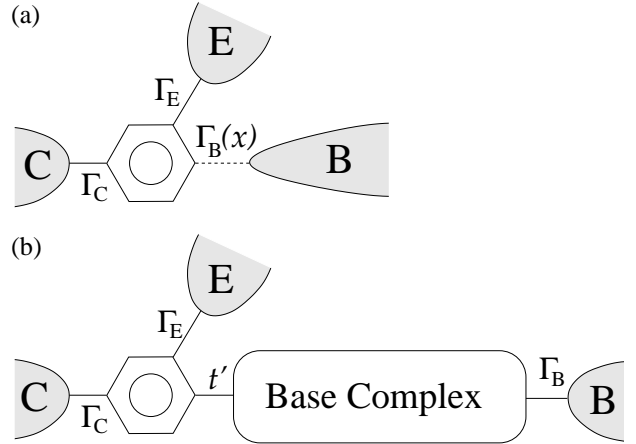


FIG. 1: Schematic diagrams of two types of QuIET. In each, base voltage modulates the coherent suppression of current between emitter (E) and collector (C) leads. In (a), base voltage controls the distance x between the benzene ring and base lead (B), for example an STM tip. This in turn controls the coupling of the ring to the base lead. In (b), a base complex is introduced between the ring and base lead. The electrostatic effect of the base lead’s bias on this molecule alters its coupling to the benzene ring.

the tunable coherent conductance suppression by which the QuIET works. Section IV focuses on the use of an acceptor-donor molecule as a scalable method of tuning interference. Section V presents numerical results which indicate the viability of this idea. Finally, Section VI contains our conclusions.

II. MODEL

The Hamiltonian of the system can be written as the sum of three terms: $H = H_m + H_l + H_{tun}$. The first is the extended Hubbard model molecular Hamiltonian

$$H = \sum_{i\sigma} \varepsilon_i d_{i\sigma}^\dagger d_{i\sigma} + \sum_{\langle ij \rangle \sigma} t_{ij} \left(d_{i\sigma}^\dagger d_{j\sigma} + \text{H.c.} \right) + \sum_{ij} \frac{U_{ij}}{2} Q_i Q_j, \quad (1)$$

where $d_{i\sigma}$ annihilates an electron on atomic site i with spin σ , ε_i are the site energies, and t_{ij} are the tunneling matrix elements. The final term of Eq. (1) contains intersite and same-site Coulomb interactions, as well as the electrostatic effects of the leads. The interaction energies are modeled according to the Ohno parameterization [1]:

$$U_{ij} = \frac{11.13\text{eV}}{\sqrt{1 + .6117 (R_{ij}/\text{\AA})^2}}, \quad (2)$$

where R_{ij} is the distance between sites i and j . Q_i is an effective charge operator for atomic site i :

$$Q_i = \sum_{\sigma} d_{i\sigma}^{\dagger} d_{i\sigma} - \sum_{\alpha} \frac{C_{i\alpha} \mathcal{V}_{\alpha}}{e} - 1. \quad (3)$$

The second term represents the polarization charge on site i due to capacitive coupling with lead α . Here $C_{i\alpha}$ is the capacitance between site i and lead α , chosen to correspond with the interaction energies of Eq. (2), and \mathcal{V}_{α} is the voltage on lead α . e is the magnitude of the electron charge.

The QuIET is intended for use at room temperature and above, a temperature range far beyond the regime in which lead-molecule or lead-lead correlations play an important role. As such, we have followed the method of Ref. [2] and treated electrostatic interactions between molecule and leads at the level of capacitance parameters. The electronic situation of the leads is thus completely determined by the externally controlled voltages \mathcal{V}_{α} , along with the leads' temperatures and Fermi energies. Each lead possesses a continuum of states, and their total Hamiltonian is

$$H_l = \sum_{\alpha} \sum_{k \in \alpha} \varepsilon'_k c_{k\sigma}^{\dagger} c_{k\sigma}, \quad (4)$$

where ε'_k are the energies of the single-particle levels k in lead α , and $c_{k\sigma}$ are the annihilation operators for the states in the leads.

Tunneling between molecule and leads is provided by the final term of the Hamiltonian:

$$H_{tun} = \sum_{\langle i\alpha \rangle} \sum_{\sigma} \left(V_{ik} d_{i\sigma}^{\dagger} c_{k\sigma} + \text{H.c.} \right). \quad (5)$$

V_{ik} are the tunneling matrix elements for moving from a level k within lead α to the nearby site i . Coupling of the leads to the ring via inert molecular chains, as may be desirable for fabrication purposes, can be included in the effective V_{ik} , as can the effect of the substituents used to bond the leads to the molecule.

A system whose Hamiltonian includes such terms as Eqs. (4) and (5) requires an infinite-dimensional Fock space, but we are concerned mainly with the behavior of the discrete molecule suspended between the leads. We therefore adopt a Green function approach, in which Dyson's Equation gives the Green function of the full system

$$G(E) = [G_m^{-1}(E) - \Sigma(E)]^{-1}, \quad (6)$$

where G_m is the Green function of the isolated molecular system. With the use of an appropriate self-energy Σ , Equation (6) is true both for the retarded Green function G^r as well as for its 2×2 Keldysh counterpart.

The retarded self-energy due to the leads is

$$\Sigma_{ij}^r(E) = -\frac{i}{2} \Gamma_i(E) \delta_{ij}, \quad (7)$$

where the energy widths are given by Fermi's Golden Rule

$$\Gamma_i(E) = 2\pi \sum_{\alpha} \sum_{k \in \alpha} |V_{ik}|^2 \delta(E - \varepsilon'_k). \quad (8)$$

We take the broad-band limit of Eq. (8) and treat each of the Γ_i as a constant parameter characterizing the lead-site coupling. The only effect of H_l and H_{tun} in this limit is to shift the poles of the Green function into the complex plane. This causes the density of states $\rho(E) = -\frac{1}{\pi} \text{Im Tr} G^r(E)$ to change from a discrete spectrum of delta functions to a continuous, width-broadened function. Due to the open nature of the system, electrons can occupy all energies.

The retarded Green function gained via Eq. (6) contains all information regarding the dynamics of the system. In particular, the current in lead β is given by the familiar multi-terminal current formula [3]:

$$I_{\beta} = \frac{2e}{h} \sum_{\alpha} \int_{-\infty}^{\infty} dE T_{\alpha\beta}(E) [f_{\alpha}(E) - f_{\beta}(E)], \quad (9)$$

where f_{α} is the Fermi function for lead α . The transmission probability is

$$T_{\alpha\beta}(E) = \Gamma_a \Gamma_b |G_{ab}^r(E)|^2. \quad (10)$$

Here $a(b)$ is the site with hopping to lead $\alpha(\beta)$. We note that Eq. (9) is an exact result of the Keldysh formalism in cases, like ours, consisting only of elastic processes.

In order to arrive at $G^r(E)$, we must consider electron-electron interactions. Here we do so via the well known self-consistent Hartree-Fock method. The Hamiltonian is replaced by its mean-field approximation

$$H_m^{\text{HF}} = \sum_{i\sigma} \left(\varepsilon_i - \sum_{j\alpha} U_{ij} \frac{C_{j\alpha} \mathcal{V}_\alpha}{e} \right) d_{i\sigma}^\dagger d_{i\sigma} + \sum_{\langle ij \rangle \sigma} t_{ij} \left(d_{i\sigma}^\dagger d_{j\sigma} + \text{H.c.} \right) + \sum_{ij\rho\sigma} U_{ij} \left(\langle d_{j\rho}^\dagger d_{j\rho} \rangle d_{i\sigma}^\dagger d_{i\sigma} - \langle d_{j\rho}^\dagger d_{i\sigma} \rangle d_{i\sigma}^\dagger d_{j\rho} \delta_{\sigma\rho} \right). \quad (11)$$

In this approximation, the retarded Green function is $G_m^r(E) = (E - H_m^{\text{HF}} + i0^+)^{-1}$.

Equation (11) gives the mean-field Hamiltonian as a function of the diagonal and off-diagonal equal-time correlation functions $\langle d_{i\sigma}^\dagger d_{j\sigma} \rangle$. To complete a self-consistent loop, we require an expression for these quantities in terms of Green functions. They are given in the Keldysh formalism by the equal-time limit of the “<” Green function

$$G_{i\sigma, j\sigma}^<(t, t') = i \langle d_{i\sigma}^\dagger(t) d_{j\sigma}(t') \rangle = \int_{-\infty}^{\infty} \frac{d\omega}{2\pi} G_{i\sigma, j\sigma}^<(\omega) e^{-i\omega(t-t')}. \quad (12)$$

From Dyson’s Equation (6) it follows [4] that

$$G^< = G^r \Sigma^< G^{r\dagger} + (1 + G^r \Sigma^r) G_m^< (1 + \Sigma^{r\dagger} G^{r\dagger}). \quad (13)$$

The second term is a purely equilibrium property, and can be related to the total charge on the molecule when the three lead biases are equal. The “<” self-energy is given by

$$\Sigma_{ab}^<(\omega) = i \Gamma_a f_\alpha(\omega) \delta_{ab}. \quad (14)$$

The desired relation between the equal-time correlation functions and G^r ,

$$\langle d_{i\sigma}^\dagger d_{j\sigma} \rangle = \sum_a \Gamma_a \int_{-\infty}^{\infty} \frac{d\omega}{2\pi} G_{i\sigma, a\sigma}^r(\omega) G_{a\sigma, j\sigma}^{r*}(\omega) f_\alpha(\omega), \quad (15)$$

is now readily computed, and the self-consistent loop is complete.

III. TUNABLE CONDUCTANCE SUPPRESSION

In the two-lead device shown in Fig. 2a, a single carrier (electron or hole) is injected into the ring by the emitter and exits via the collector some time later. In the path integral formulation of quantum mechanics, it traverses all paths around the ring allowed by the connectivity of the system during this process.

We operate the QuIET in the regime where there is little charge transfer between it and the leads. In the linear response, the carrier has momentum equal to the Fermi momentum of the ring $k_F = \frac{\pi}{2a}$, where $a = 1.397\text{\AA}$ is the intersite spacing of benzene. Clearly, then, the phase difference between paths ① and ② is π , and they cancel exactly. Similarly, all of the paths through the ring from emitter to collector exactly cancel in a pairwise

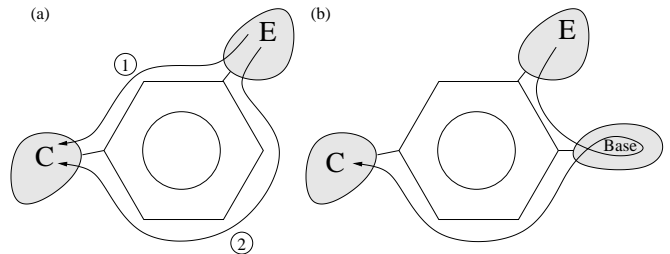


FIG. 2: (a) Two-lead experiment to measure the conductance of benzene when the leads are in the meta configuration. Shown are the two most direct paths a carrier can take from the emitter lead to the collector. These two cancel exactly, as do all other paths with the same endpoints in a similar pairwise fashion. (b) Example of a new path allowed when a base complex or lead is included. Such paths are not canceled, and so contribute to the total current between emitter and collector.

fashion. Therefore, transport of carriers is forbidden in linear response.

It is a consequence of Luttinger’s Theorem [5] that this coherent suppression of current persists into the interacting regime, as demonstrated in Fig. 3a. The transmission is calculated by the self-consistent Hartree-Fock model outlined in Section II. In this figure the base coupling $\Gamma_B = 0$, and so transmission at the Fermi energy is wholly suppressed by coherence. Figure 3b shows how this result changes as Γ_B is increased. Current is allowed to flow due to two new phenomena. The first is that new paths, such as the one shown in Fig. 2b, are added. These paths have no particular phase relationship to other paths, and so support transmission. Additionally, nonzero Γ_B denotes decoherence, and therefore a departure from the perfect coherent current suppression of $\Gamma_B = 0$. This is the basic operating principle of the QuIET: coherent current suppression can be tunably broken by the introduction of decoherence and dephasing from a base complex or third lead. In fact, Figure 3c shows that the transmission varies nearly linearly for $\Gamma_B \leq t$.

Clearly, the transistor behavior based on the mechanism outlined above is requisite upon an assumption that the device be operated well within the gap of benzene. The numerical simulations discussed in Section V indicate that the best transistor results are found for collector-emitter bias $\lesssim 1-2\text{V}$. Another, related, consideration is that in equilibrium, charge transfer between the molecule and leads not play an important role. For this

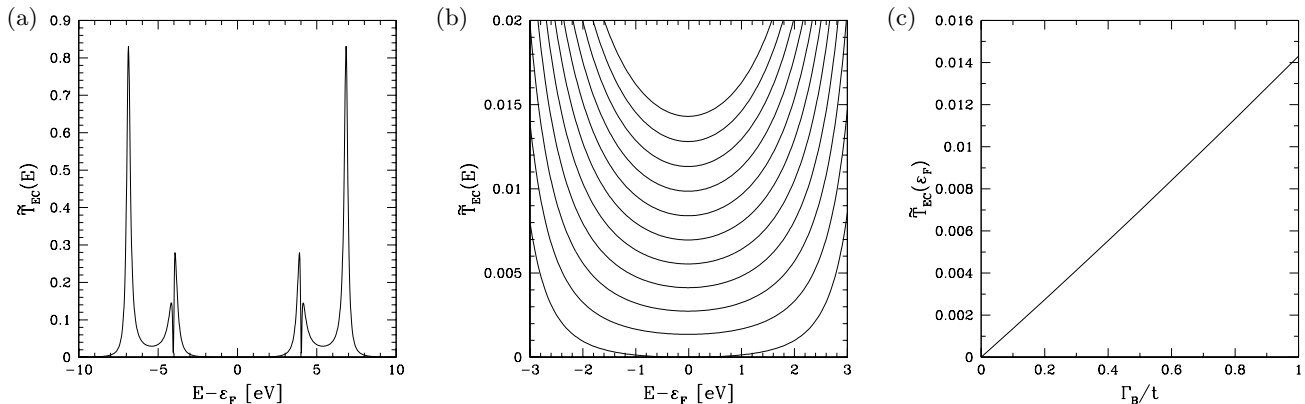


FIG. 3: Total transmission probability of the device shown in Fig. 1a. $\tilde{T}_{EC} = T_{EC} + \frac{T_{EB}T_{BC}}{T_{EB}+T_{BC}}$, where the second term is due to a restriction that the base lead be an infinite-impedance ideal voltage probe [6]. Here, $\Gamma_E = .5t$ and $\Gamma_C = .2t$, but the choice of energy widths does not affect the qualitative results. In (a), $\Gamma_B = 0$. In (b), the lowest curve shows $\Gamma_B = 0$ and each successive curve shows increasing Γ_B in increments of $.1t$. (c) shows the transmission at the Fermi energy as a function of Γ_B .

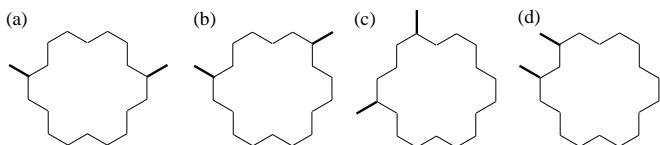


FIG. 4: Emitter-collector lead configurations possible in a QuIET based on [18]-annulene. The bold lines represent the positioning of the two leads. Each of the four arrangements has a different phase difference associated with it: (a) π , (b) 3π , (c) 5π , and (d) 7π .

to be true, the work function of the metallic leads must be comparable to the chemical potential of benzene. Fortunately, this is the case with many bulk metals, among them palladium, iridium, platinum, and gold [7].

While in this work we have chosen to focus on benzene, the QuIET mechanism applies to any aromatic annulene with leads positioned so the two most direct paths have a phase difference of π . Furthermore, larger molecules have other possible lead configurations, based on phase differences of 3π , 5π , etc. Figure 4 shows the lead configurations for a QuIET based on [18]-annulene. Of course, benzene provides the smallest of all possible QuIETs.

The position of the third lead affects the degree to which destructive interference is suppressed. For benzene, the most effective location for a third lead is shown in Fig. 5a. The base may also be placed at the site immediately between the emitter and collector leads, as shown in Fig. 5b. The QuIET operates in this configuration as well, although since base coupling to the current carriers is less, the transistor effect is somewhat suppressed. The third, three-fold symmetric configuration of leads (Fig. 5c) completely decouples base from current carriers within benzene. Because of this, the base cannot be used to provide the decoherence or dephasing neces-

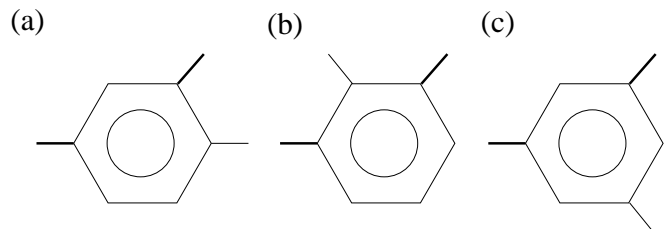


FIG. 5: The three different arrangements for a third lead on benzene when the emitter and collector leads (bold) are in the meta configuration. (a) is the choice which couples most strongly to the conducting orbitals of benzene. (b) is a second case which allows for QuIET operation. The third possibility, (c), decouples entirely from the conducting molecular orbitals by symmetry. A third lead in this configuration cannot break the coherent current suppression at all, and so the molecule does not function as a QuIET.

sary to QuIET operation in this configuration. For each aromatic hydrocarbon, exactly one three-fold symmetric lead configuration exists and yields no transistor behavior.

IV. BASE COMPLEX

With the tunable current suppression outlined in the previous section, the working principle of a transistor has become apparent. The most straightforward method of varying Γ_B is to change the distance of the third lead from the hydrocarbon molecule, as via an STM tip. It is also possible, however, to interpose an additional molecular complex between annulene and the base lead. If the effect of biasing the base lead is to increase the transparency of the molecular complex, dephasing and decoherence result. Such a QuIET is depicted schematically

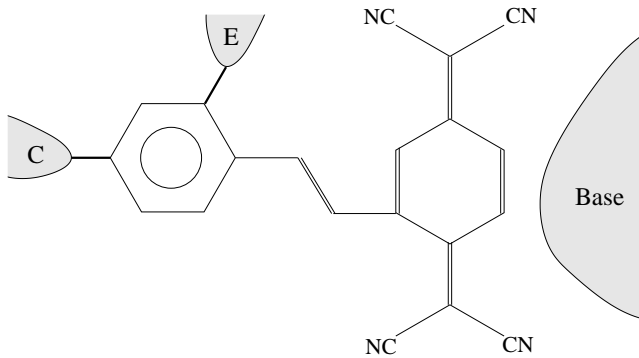


FIG. 6: Specific example of a QuIET: a dithiol derivative of phenylene–TCNQ. E and C are the emitter and collector leads. The base lead can be either weakly coupled via TCNQ, as for a BJT analogue, or capacitively coupled if FET-like behavior is desired.

in Fig. 1b.

A simple way to engineer the base complex is to include two spatially separated orbitals, with a detuning from each other Δ and hopping to each other t_B . If $\Delta \gg t_B$ for zero bias on the base lead, paths through the base complex are highly suppressed. Since the orbitals are spatially separate, however, one electrostatically couples more strongly to the base lead. Thus, the voltage on that lead can be used to control Δ , and hence change the transparency of the base complex. The result is the broad conductance peak characteristic of two discrete levels coming into resonance.

One way to achieve this structure is simply to link the annulene via an inert bridge to a donor or acceptor molecule, *e. g.* the dithiol derivative of phenylene–TCNQ shown in Fig. 6. In this case, the effect of a base bias of appropriate sign is to bring the lowest unoccupied molecular orbital (LUMO) of TCNQ into resonance with the neighboring π orbital of phenylene. The extra paths allowed within and through the TCNQ break the coherent suppression of current within the benzene ring. Any donor or acceptor molecule with which phenylene bonds in this way will yield similar results, although a donor used in this way will allow emitter-collector current to flow for negative, rather than positive, base voltages.

The class of donor-acceptor rectifiers proposed by Aviram and Ratner [8] have this two-level structure as well. These molecules possess an orbital of increased electron affinity (the acceptor) and one of increased ionization potential (the donor), as well as perhaps an inert bridge orbital. By the influence of a base lead, the donor highest occupied molecular orbital (HOMO) and acceptor LUMO can be brought into resonance, and the rectifier be made to serve as an effective QuIET base complex. In addition to this effect, several many-body mechanisms have been proposed whereby such molecules could exhibit asymmetric current flow [9]. For our purposes, however, it is sufficient to note that rectification in general is indicative of a tunable transparency to charge carriers.

TABLE I: Approximate ranges of values available for molecular diodes which could be used as QuIET base complexes.

Parameter	Range
Donor HOMO energy	[-8,-5]eV
Acceptor LUMO energy	[-3,-1]eV
t_B	[.01,1]eV
t'	[.01,1]eV
Distance between donor and acceptor	[6,10]Å

The variety within this well studied family of molecules (*e. g.*, Refs. [8, 9, 10, 11, 12, 13]) lends a great deal of versatility to the QuIET. Different choices of donor, acceptor, and bridge molecules allow QuIETs to be fabricated for specific applications. Table I gives approximate ranges of parameters available for the use of molecular diodes as base complexes.

V. NUMERICAL RESULTS AND DISCUSSION

We turn now to discussion of numerical results, based on the self-consistent Hartree-Fock model presented in Section II. For the purposes of illustration, the numerical results are based on the dithiol derivative of phenylene–TCNQ shown in Fig. 6 and three bulk gold leads. Similar results can be obtained for many such QuIETs.

For the purposes of electrostatic interactions, each lead is considered to be immediately adjacent to its neighboring site. The electrostatic interactions between TCNQ and phenylene are modeled as those between two conducting spheres of appropriate size, while within phenylene the Ohno parameterization (2) is used. We neglect reduction of the U_{ij} due to screening from a third site, an effect which we find to be of the order of 1%. In keeping with our assumption that the leads do not significantly perturb the molecular system, modifications to the interaction parameters due to the presence of the leads are also neglected.

A typical $I - \mathcal{V}$ diagram for this QuIET is shown in Fig. 7, demonstrating that the QuIET is quite reminiscent in operation to classical transistors. The currents in the emitter and collector leads exhibit a broad resonance as the base voltage is increased. Furthermore, for nonzero Γ_B , the device amplifies the current in the base lead, providing emulation of the classical BJT. Since a donor, TCNQ, was used in the base complex, the device performs in a manner analogous to an NPN transistor, with base current flowing into the molecule. Use of an acceptor instead, for example TTF, yields PNP-like behavior. For capacitive coupling of the third lead, on the other hand, a FET-like $I - \mathcal{V}$ characteristic is obtained.

We interpret this transistor behavior as due to the coherence mechanism discussed in Section III. If hopping between the benzene ring and the base complex is set to zero, we find that full coherent current suppression is re-

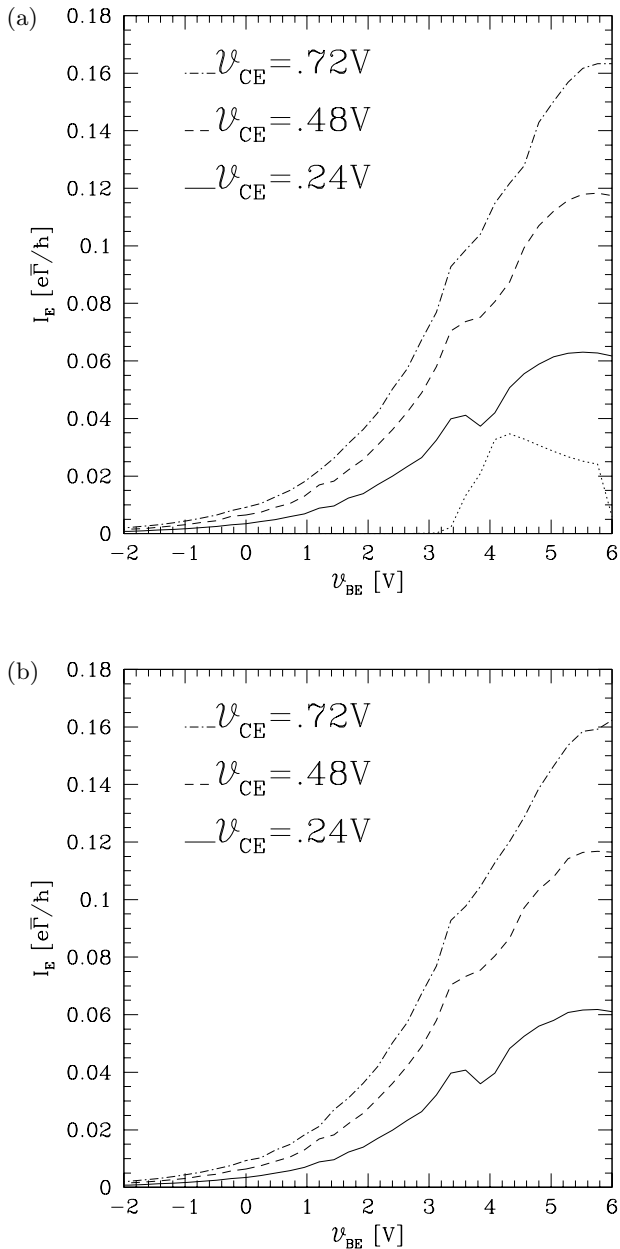


FIG. 7: Typical $I - V$ characteristic of two QuIETs, showing emitter current out of the molecule vs. voltage on the base lead for three different biases applied to the collector, with the emitter ground. The calculation is done for the molecule in Fig. 6 at room temperature. $\bar{\Gamma} \equiv \frac{\Gamma_E \Gamma_C}{\Gamma_E + \Gamma_C}$ gives the sequential tunneling rate through the device. Here, $\Gamma_E = \Gamma_C = 2.4\text{eV}$. In (a), $\Gamma_B = .0024\text{eV}$, and the QuIET amplifies current, similar to a BJT. The dotted curve is the base current into the molecule for the case of $V_{CE} = .24\text{V}$, multiplied by 10 for clarity. Base currents for other collector voltages are similar. (b) shows the FET limit of the QuIET, with $\Gamma_B = 0$.

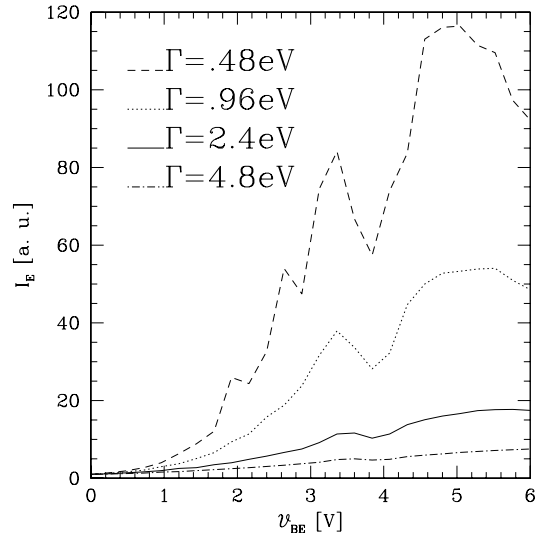


FIG. 8: I_E vs. V_{BC} for different values of $\Gamma_E = \Gamma_C = \Gamma$. Each curve has been scaled so that the leakage current at zero bias is 1. $\Gamma_B = 0$, $V_{CE} = .24\text{V}$, and positive current is out of the molecule. Reducing Γ suppresses the leakage current, but does not strongly affect the QuIET's behavior on-resonance, thus greatly enhancing its overall function.

stored and almost no current flows between the emitter and collector leads. Furthermore, the current step effect persists for arbitrarily small Γ_B , which is consistent with our interpretation that transport through the non-canceling paths is enhanced by the electrostatic effect of the third lead.

Estimation of the Γ_i 's remains an open question in the field of molecular electronics. Similar quantities are often estimated to be $\lesssim .5\text{eV}$ [14, 15] by the method of Ref. [16], whereas values as high as 1eV have been suggested [17]. For the emitter and collector broadenings, we have taken values somewhat higher than the norm for the sake of numerical convergence. Fortunately, nothing in the arguments of Sections III or IV depends strongly on the choice of these quantities. So long as they are positive, their magnitude merely determines the scale of the current, and has negligible effect on the overall operating principle and transistor behavior of the QuIET.

Figure 8 demonstrates the effect of varying the coupling of the benzene ring to emitter and collector leads. As is to be expected, the internal structure of the resonance, due to electrons moving to screen the changing field from the base, sharpens. Furthermore, at low base voltages, less than about $.75\text{V}$, the base complex is strongly off resonance, and the scale of the leakage current through the annulene is set mainly by $\bar{\Gamma} \equiv \frac{\Gamma_E \Gamma_C}{\Gamma_E + \Gamma_C}$, an expected result for systems like the QuIET, which are not near a charge fluctuation resonance [18].

For higher base voltages, the base complex begins to play an important role. Thus, as described by Ref. [15],

$\bar{\Gamma}$ alone no longer determines the scale of the current. Instead, we find that the rate-limiting process is travel through the base complex, and varying Γ_E and Γ_C has little effect. Thus, smaller emitter and collector energy widths enhance the QuiET's current contrast dramatically.

VI. CONCLUSIONS

We have presented a novel idea for a small single-molecule transistor. The device is based on the coherent suppression of current through an aromatic hydrocarbon ring, and the control of that effect by increasing the contribution of paths outside the ring. Two simple methods of creating that control, either through an STM tip or

through a small base complex, were discussed, and numerical results presented.

In contrast to SET-style devices, the QuiET is predicted to be an extremely versatile, scalable device. Since it is chemically constructed, it should be possible to fabricate as many identical QuiETs as desired. Furthermore, QuiETs can be designed which mimic the functionality of all major classes of macroscale transistors: FET, NPN, and PNP.

Acknowledgments

The authors acknowledge support from National Science Foundation Grant Nos. PHY0210750, DMR0312028, and DMR 0406604.

-
- [1] K. Ohno, *Theor. Chim. Acta* **2**, 219 (1964); M. Chandross *et al.*, *PRB* **55**, 1486 (1997).
 - [2] C. A. Stafford, R. Kotlyar, and S. Das Sarma, *PRB* **58**, 7091 (1998).
 - [3] M. Büttiker, *Phys. Rev. Lett.* **57**, 1761 (1986).
 - [4] A.-P. Jauho, N. S. Wingreen, and Y. Meir, *PRB* **50**, 5528 (1994).
 - [5] J. M. Luttinger, *Phys. Rev.* **119**, 1153 (1960).
 - [6] S. Datta, *Electronic Transport in Mesoscopic Systems*, Cambridge University Press, Cambridge (1995).
 - [7] D. R. Lide, *et al.*, eds., *CRC Handbook of Chemistry and Physics*, CRC Press, Boca Raton, Fla. (2005).
 - [8] A. Aviram and M. Ratner, *Chem. Phys. Lett.* **29**, 277 (1974).
 - [9] D. H. Waldeck and D. N. Beratan, *Science* **261**, 576 (1993).
 - [10] N. J. Geddes *et al.*, *App. Phys. Lett.* **56**, 1916 (1990).
 - [11] R. M. Metzger *et al.*, *J. Am. Chem. Soc.* **119**, 10455 (1997).
 - [12] R. M. Metzger *et al.*, *J. Phys. Chem.* **B107**, 1021 (2003).
 - [13] J. R. Heath and M. A. Ratner, *Physics Today* **56**(5), 43 (2003).
 - [14] A. Nitzan, *Annu. Rev. Phys. Chem.* **52**, 681 (2001).
 - [15] M. Paulsson, F. Zahid, and S. Datta, in *Handbook of Nanoscience, Engineering, and Technology*, W. A. Goddard III *et al.*, eds., CRC Press, Boca Raton, Fla. (2003).
 - [16] V. Mujica, M. Kemp, and M. A. Ratner, *J. Chem. Phys.* **101**, 6849 (1994).
 - [17] W. Tian *et al.*, *J. Chem. Phys.* **109**, 2874 (1998).
 - [18] C. A. Stafford, *Phys. Rev. Lett.* **77**, 2770 (1996).